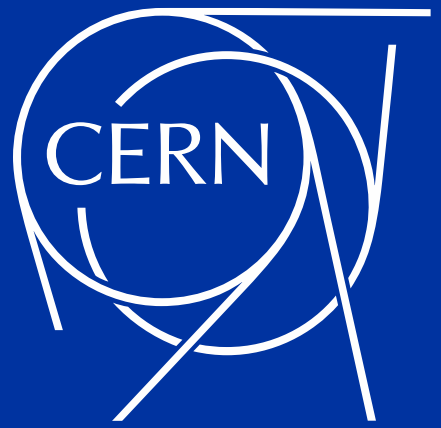

Room Temperature Magnetic Measurements of the HL-LHC Corrector Package

TM Science

Eivind Dalane
Supervisor: Carlo Petrone

03.05.2022

Outline

- **The HL-LHC Corrector Package**
- **Measurement Requirements**
- **Available Measurement Methods**
- **Challenges**
- **Proposed Measurement Procedure**
  - Single Stretched Wire with magnet in AC mode
    - Validation measurements
  - Translating fluxmeter
    - Validation measurements
- **Next Step**

The HL-LHC Corrector Package

- Ad hoc correction of residual field quality of the inner triplet and separation-recombination dipoles.
- Nested Dipole Correctors (green in the figure):
  - Generate crossing angle.
  - Correct misalignment and strength errors in Q1-Q3.
- Higher Order Correctors (red in the figure):
  - Compensate the field quality effects of the triplets and separation dipoles (D1 & D2):
    - Cancel resonance driving terms for both cw. and ccw. rotating beam for any given normal or skew imperfection.
    - Correct the triplet tilt.
- Super-ferric technology: Nb-Ti strands.

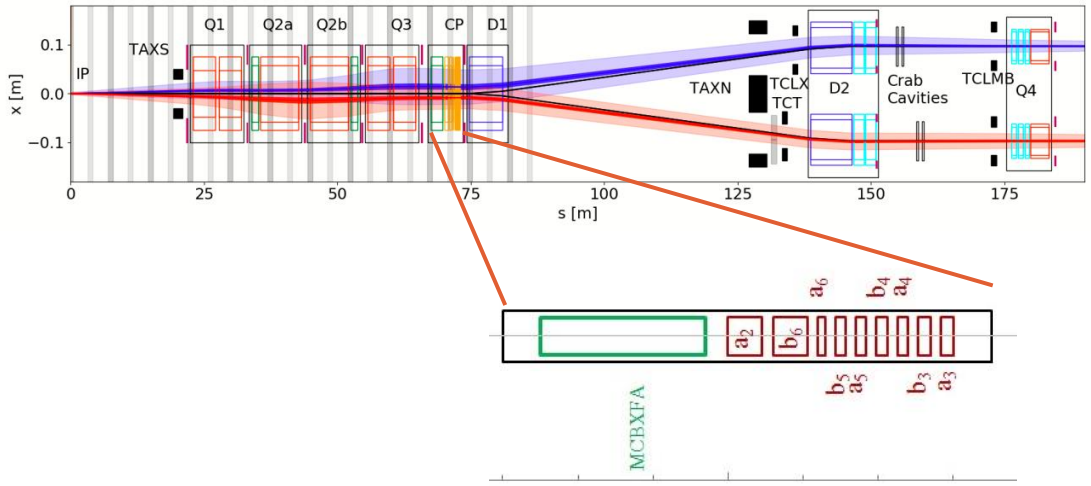

Measurement Requirements

- Cold measurements: **field quality.**
- Warm measurements: **magnetic axis**, **roll angle** and **longitudinal field profile** for validation of positioning.

Warm Measurement Uncertainty Requirements at 3σ			
Transverse centre [mm]	Roll [mrad]	Long. Centre [mm]	Mag. Length [mm]
0.4	0.3	10	10

Available Measurement Methods

- **Longitudinal profile:**
  - Mapping with Hall probes
  - Scan with Rotating Coils
  - Harmonic Coil in AC mode
  - Fluxmeters
- **Magnetic axis and roll angle:**
  - Rotating Coil
  - Single Stretched Wire (SSW)
  - Vibrating Wire (VW)
  - Oscillating Wire (OW)

Wire Measurements (I)

Single-Stretched Wire
The voltage induced along the stretched wire is obtained by

$$\int_{t_1}^{t_2} U \; dt = \int_{\partial\mathcal{A}} \boldsymbol{B}\, \hat{\mathbf{n}}\, da\,,$$

when it is moved within the aperture of the magnet.

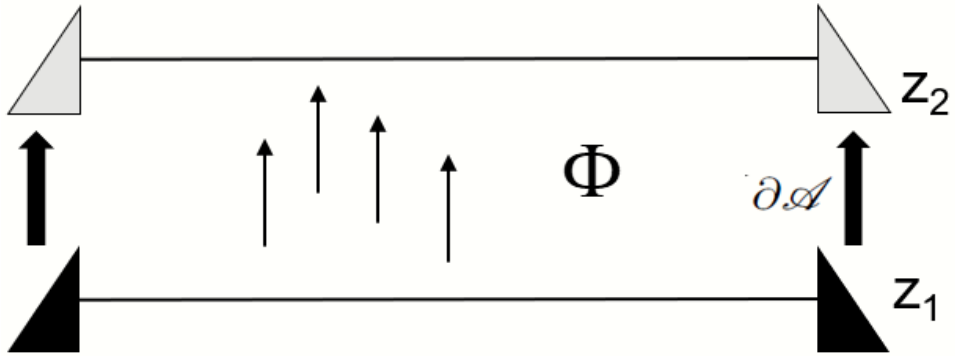

The voltage is integrated to yield the total flux change by the change of the area spanned by the wire.

Vibrating Wire
Wire powered by an AC current. This gives a vibration of the wire according to:

$$F = q \cdot (\boldsymbol{E} + \boldsymbol{v} \times \boldsymbol{B})$$

The amplitudes of the wire are measured by photo-transistors.

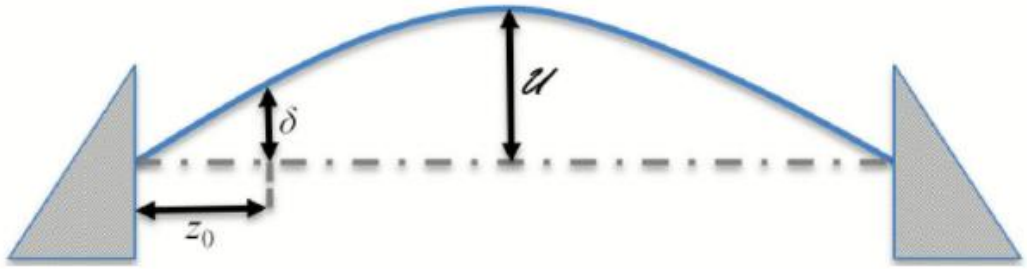

Wire Measurements(II)

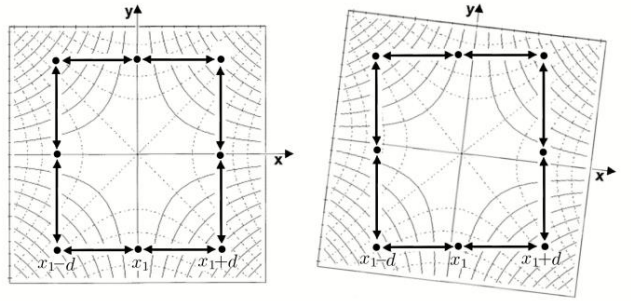

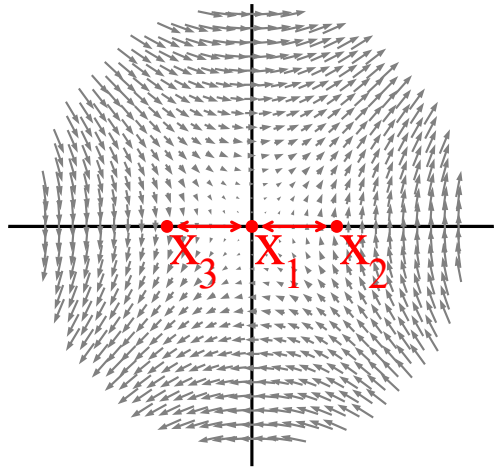

Localization of axis and roll angle

Single-Stretched Wire:
1) Utilizing **field symmetry** around axis.
2) Circular trajectory with following harmonic analysis.

Vibrating Wire:
Analysis of vibration of wire at different positions, finding the axis where the vibration of the first resonance mode is zero.

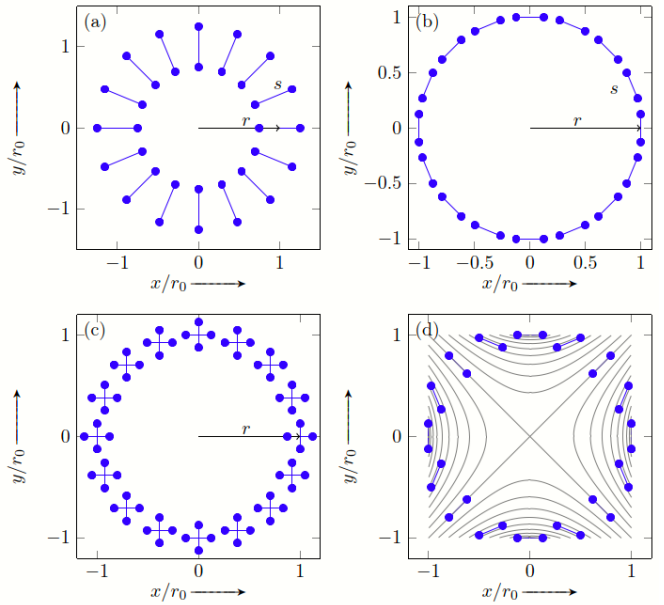

Challenges

- Room temperature measurement gives **low field values**.
- The **gradients** of higher order corrector magnets are **flat** around the axis.
- Difficult to **position** the rotating coils w.r.t. the fiducials.
- We want to have the longitudinal field profile of the entire package.

Proposed Method: Main ideas

- Use the **Single Stretched Wire**, with the magnets powered in AC mode, as a “radial harmonic coil” to consecutively measure the magnetic axis and roll angle of the corrector magnets.
  - Increased signal-to-noise ratio.
  - No remanence field bias.

- Development of a **translating fluxmeter** for acquiring the longitudinal field profile
  - Simple and little time-consuming.
  - Detailed measurement of field strength along the beam trajectory in several azimuthal positions.

Single Stretched Wire Measurement Setup

- **Wire Stages**: Pi miCos® HPS-170, abs. position accuracy ± 0.1 µm, repeatability ± 0.1 µm, encoder resolution 50 nm
- **Optical Sensor**: Sharp® GP1S094HCZ0F
- **Copper-Beryllium (Cu-Be) Wire**: Ø 0.125 mm
- **FDI**: $f_s = 1024$ Hz, $f_{int} = 500$ kHz
- **Power Supply**: 6221 Keithley® AC and DC Current Source, $\hat{I} = 105 \pm 0.001$ mA, Offset ± 0.4 mA, $f_{PS} = 23 \pm 0.0023$ Hz

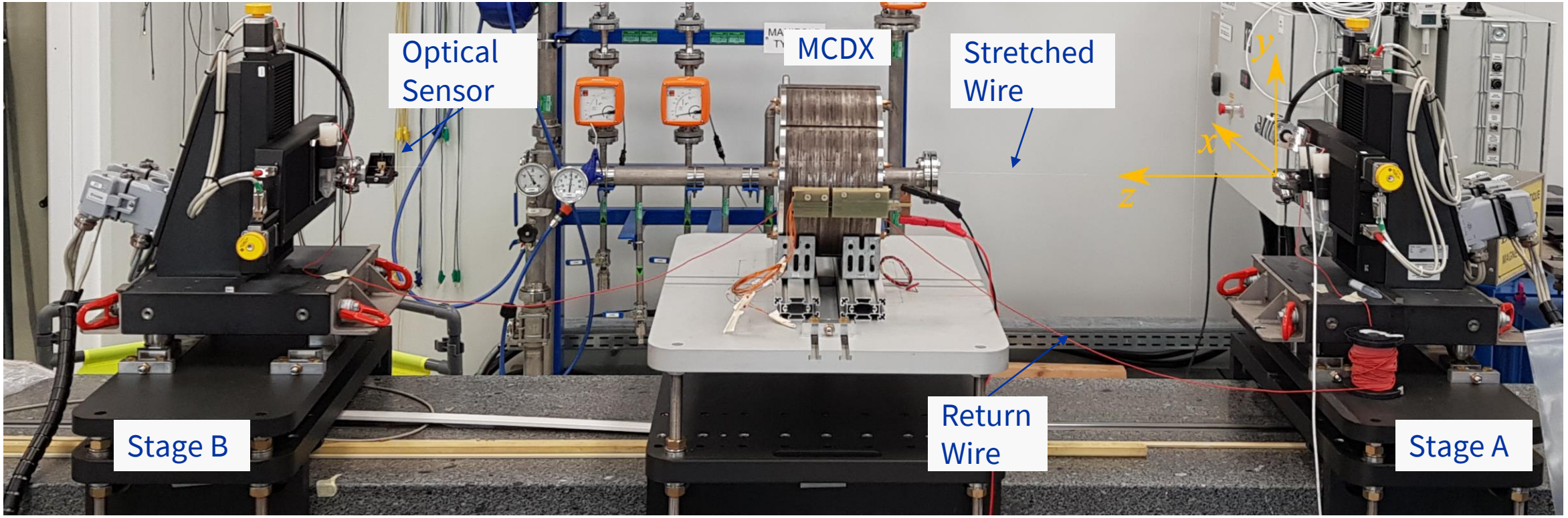

Proposed Method: Single Stretched Wire Analysis (I)

- **Basic Principle:**
  We measure with the magnet powered by an **AC current** the induced voltage for ***t* seconds** at **N+1 points;** The center and N along the circumference of the aperture.

  The N measurements are subtracted from the central measurement to mimic a **radial search coil**:

$$\Phi(t) = -\mathrm{N}l\, Re\left\{\int_{z_1}^{z_2} \boldsymbol{B}(z)dz\right\} = -Re\left\{\sum_{n=1}^{\infty} C_n(r_0)S_n^{rad}(r_0)e^{in(\varphi-\frac{\pi}{2})}\right\},$$

$$S_n^{rad} = \frac{2Nlr_0}{n}\left[\left(\frac{r_2}{r_0}\right)^n - \left(\frac{r_1}{r_0}\right)^n\right]$$

N: Number of turns,
l: Lenght of coil,
S_n^{rad}: Complex sensitivity factor for radial coils

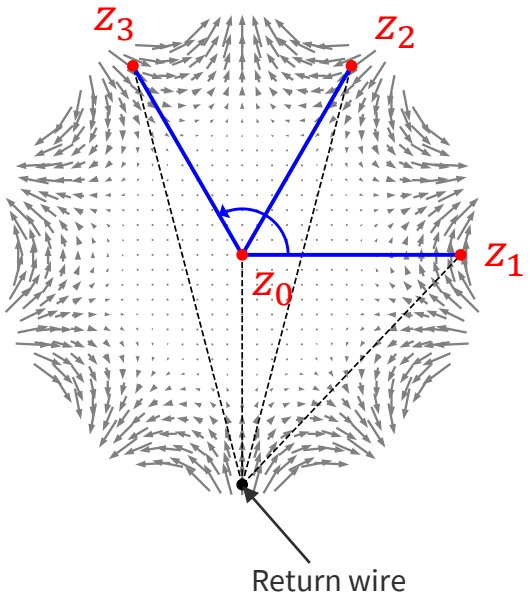

$$\Phi_{z_1 z_0} = \Phi_{z_1} - \Phi_{z_0}$$

  We then perform a **spatial Fourier Analysis** on the measured values.

Proposed Method: Single Stretched Wire Analysis (II)

- **Measurement and Setup**
  - The magnet is powered in AC mode .
    - Induced signal increased by a factor f_{PS}, since $\mathrm{d}\Phi/\mathrm{dt} \sim f_{PS}$.
    - No remanence field bias.
  - $\hat{\mathrm{I}} = 105\ \mathrm{mA} < 200\ \mathrm{mA} = \mathrm{I}_{\mathrm{max}}$.
  - $f_{PS} = 23\ \mathrm{Hz}$: Avoid any $50\ \mathrm{Hz}$ harmonics and optimize the signal-to-noise ratio of the signal.
  - The wire is moved in a circular trajectory of N points, in addition to the center.
    - $\mathrm{N} = 128$: optimum to reduce the measurement time and to maintain a circular trajectory of the wire.
    - r_{meas}: as large as possible, due to the high gradient of the field.
  - In each position the induced voltage is measured and integrated in the FDIs for $t = 4$ seconds.

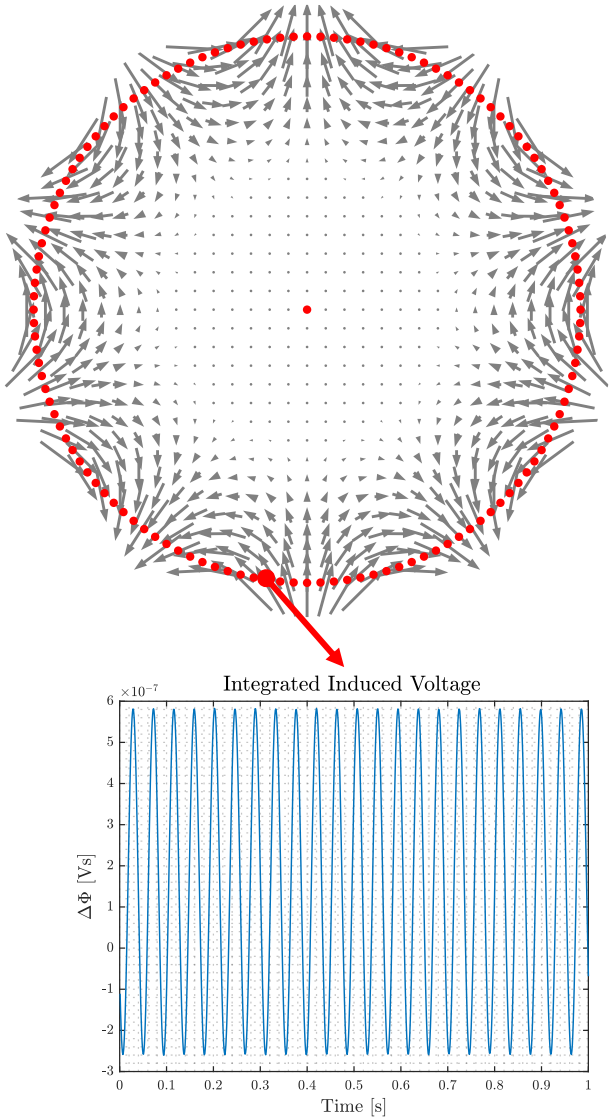

Proposed Method: Single Stretched Wire Analysis (III)

- **Post-Processing of Acquired Signals**

1. The Φ(t)-signals are analyzed to find the amplitude of the f_{PS}-frequency signal by Fourier Analysis of the time-dependent signal.
2. The amplitudes are assigned to the spatial position, $\Phi(\theta, r_{meas})$.
3. The measurement in the center , $\Phi(0,0)$, is subtracted from all the circumferential measurements to obtain the value measured by a radial coil. (Figure A)
4. We get the values for C_n by a Fourier Analysis of the sampled values of $\Phi(\theta, r_{meas})$ along the circular wire trajectory.

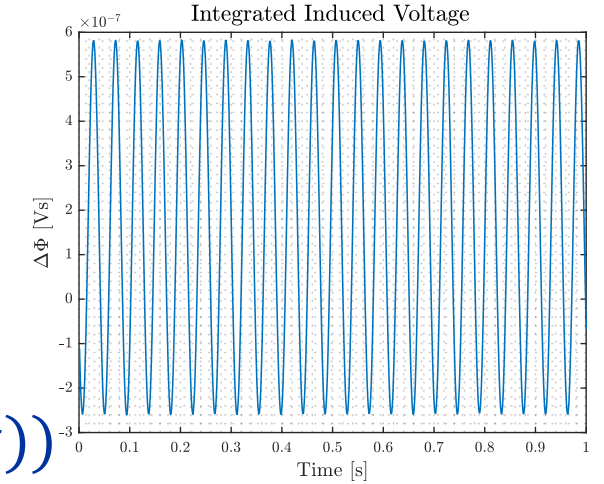

$FFT(\Phi(t))$

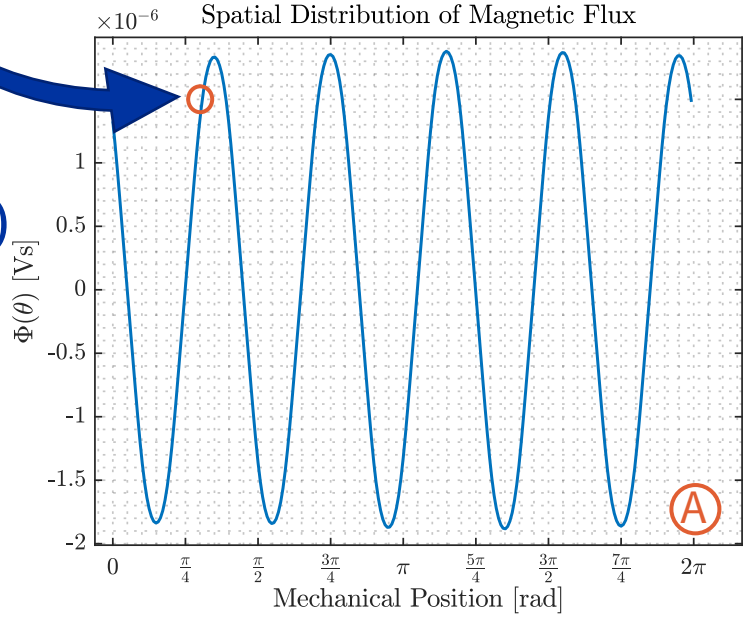

$FFT(\Phi(\theta, r_{meas}))$

$$\boldsymbol{B}(z) = \sum_{n=1}^{\infty} C_n(r_0) \left(\frac{z}{r_0}\right)^{n-1}$$

Proposed Method: Single Stretched Wire Analysis (IV)

- **Multipole Coefficients Analysis**
  - The roll angle is found as the angle between A_N and B_N, where N is the main multipole component, defined as

$$\tan\varphi = \frac{A_N}{B_N}, \qquad \left[-\frac{\pi}{2}, \frac{\pi}{2}\right]$$

  - We get the displacement of the measurement axis from the magnetic axis, $z_d = x_d + iy_d$, from the feed-down

$$z_d = -\frac{r_0}{N-1}\frac{C_{N-1}}{C_N}.$$

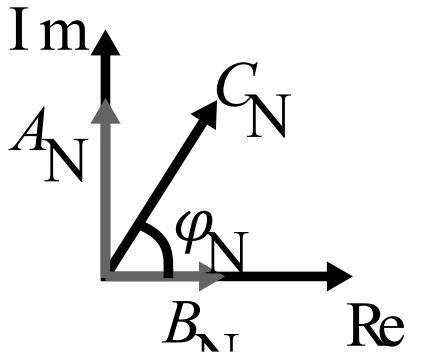

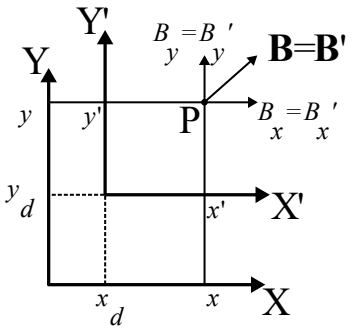

- **Wire Sag Correction**
  The sag of the Cu-Be wire is calculated as

$$y_g = \frac{g}{2}\cdot\left(\frac{\pi}{\omega_1 L}\right)^2 \cdot s^2 + \frac{1}{s_B}\left(y_A - y_B - \frac{g}{2}\cdot\left(\frac{\pi}{\omega_1 L}\right)^2 s_B^2\right)\cdot s + y_A$$

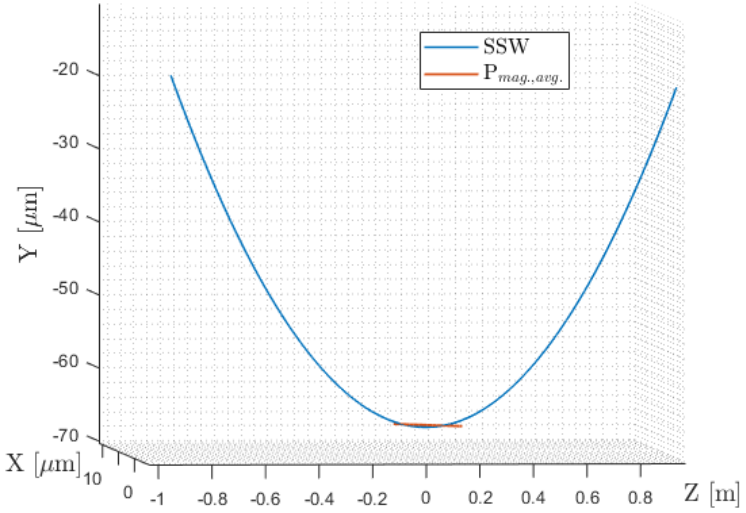

SSW Analysis: Validation Measurements (I)

- **Displacement of the Magnetic Axis**
  - How well can we measure a precisely imposed displacement of the measurement axis?
  - Relative displacement per position*: $\Delta x_i = \Delta z_i - \Delta z_0$.
  - The **precision:** How well the measured Δx corresponds to known displacement of stages.
- **Next step**:
  Determine the **accuracy:** compare it to vibrating wire measurement of the quadrupole corrector.

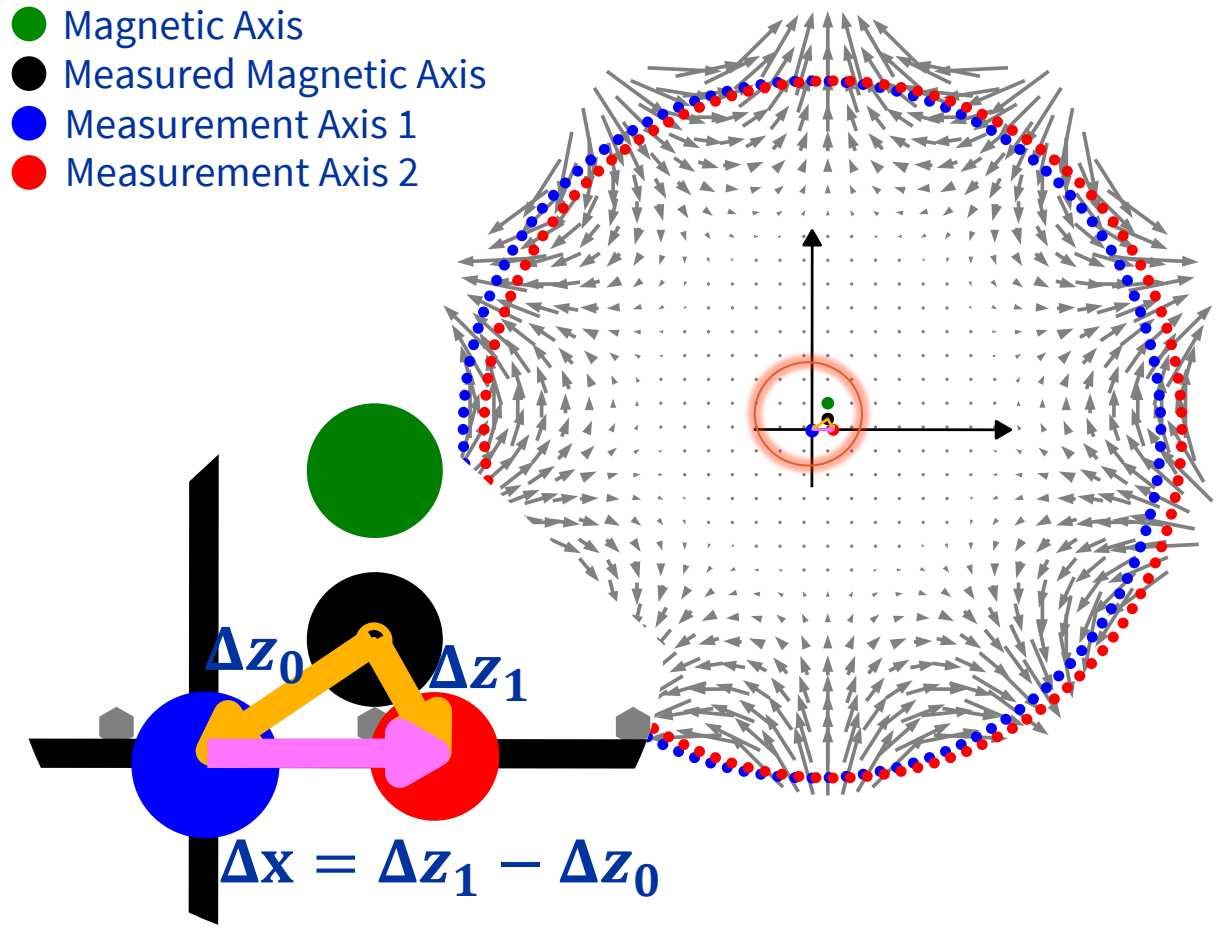

*For simplicity, a pure horizontal displacement is shown here. However, the same principle applies to any displacement in the x-y-plane.

SSW Analysis: Validation Measurements (II)

Results:
Relative displacement in both x- and y-direction, with arbitrary step size.

- **Red dots**: measured displacement with the SSW.
- **Blue circle**: displacement measured by the encoders of the stages.

The same results are shown in the lowermost table on the next slide.
The uppermost table shows another set of displacement measurements, with displacements in x- and y-direction separately, and with larger step sizes.

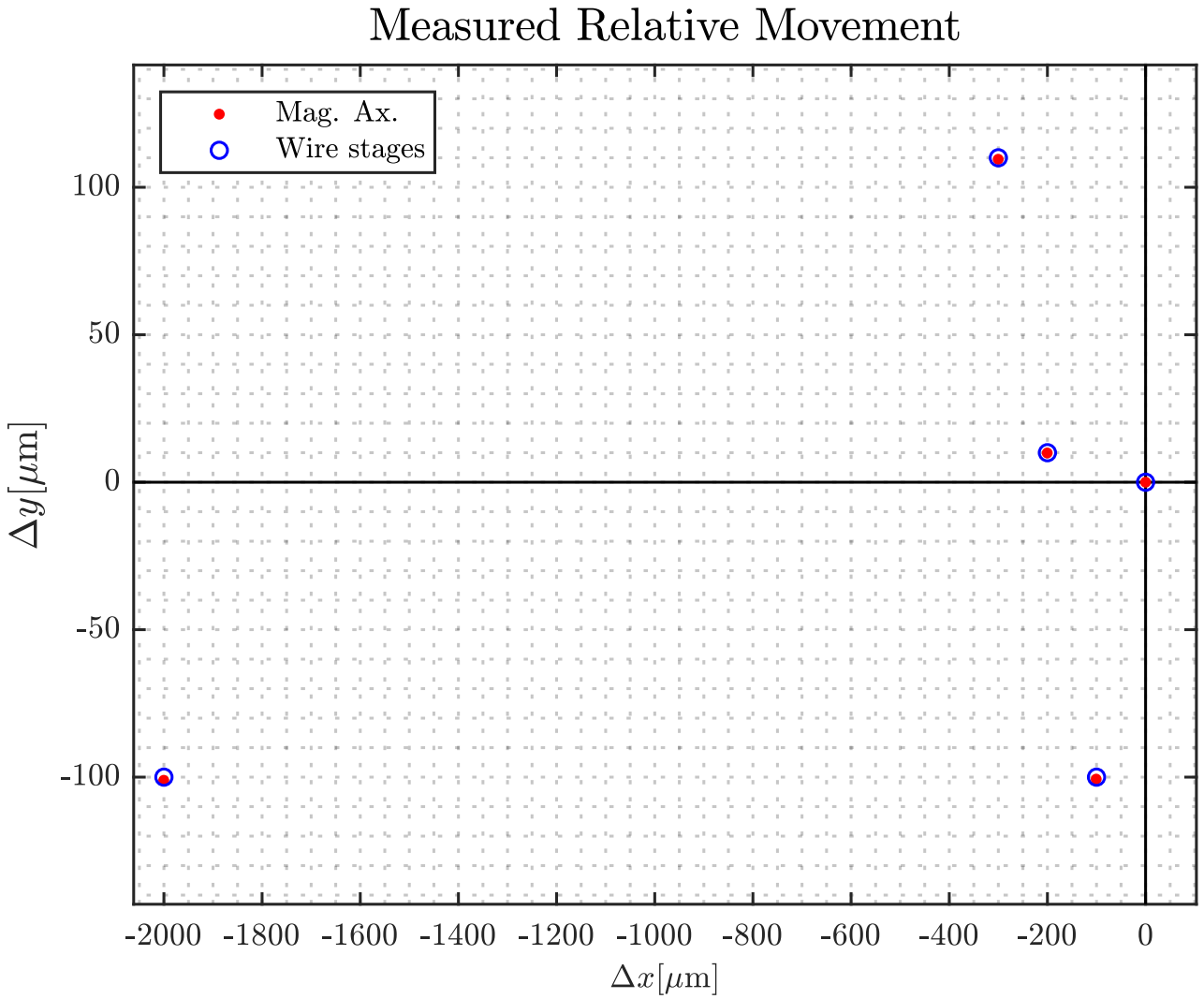

SSW Analysis: Validation Measurements (III)

$\Delta x_s, \Delta y_s$: Displacement of initial wire position determined by the *stages*
$\Delta x_m, \Delta y_m$: *Measured* displacement of initial wire position.

$(\Delta x_s, \Delta y_s) \pm 3\sigma$ [μm]	$(1000,0) \pm 3$	$(2000,0) \pm 3$	$(4000,0) \pm 3$	$(0,1000) \pm 3$	$(0,2000) \pm 3$	$(0,4000) \pm 3$
$\Delta x_m \pm 3\sigma$ [μm]	1000.0 ±1.5	2000.2±2.0	4000.8±1.8	0.2±1.7	0.3±1.5	-0.4±**3.8**
$\Delta y_m \pm 3\sigma$ [μm]	0.0±1.7	0.4±1.7	0.1±1.3	999.8±3.0	2000.8±2.9	4000.4±2.7
$\lvert\Delta x_m - \Delta x_s\rvert$ [μm]	0.0	0.2	0.8	0.2	0.3	0.4
$\lvert\Delta y_m - \Delta y_s\rvert$ [μm]	0.0	0.4	0.1	0.2	0.8	0.4

$(\Delta x_s, \Delta y_s) \pm 3\sigma$ [μm]	$(-100,-100) \pm 3$	$(-2000,-100) \pm 3$	$(-200,10) \pm 3$	$(-300,110) \pm 3$
$\Delta x_m \pm 3\sigma$ [μm]	-100.7±1.0	-2000.4±1.3	-200.4±1.6	-300.3±1.4
$\Delta y_m \pm 3\sigma$ [μm]	-100.7±1.8	-101.1±2.6	9.9±1.5	109.5±1.7
$\lvert\Delta x_m - \Delta x_s\rvert$ [μm]	0.7	0.4	0.4	0.3
$\lvert\Delta y_m - \Delta y_s\rvert$ [μm]	0.7	**1.1**	0.1	0.5

SSW Analysis: Validation Measurements (IV)

- **Roll Angle Measurement**
  - We need to know how well we can locate an imposed roll angle with the measurement procedure.
  - This is tested by rotating each measurement point by a fixed angle, α_{imp}, corresponding to a physical rotation of the poles by $-\alpha_{imp}$, and see how well the measured flux correspond to this.

$\boldsymbol{\varphi_0 \pm 3\sigma}$ **[mrad]**	154.015±0.079
$\boldsymbol{\alpha_{imp}}$**[mrad]**	-160.1±0.03
$\boldsymbol{\varphi_m \pm 3\sigma}$ **[mrad]**	-6.073±0.022
$\boldsymbol{\Delta\varphi \pm 3\sigma}$**[mrad]**	160.088±0.082

- **Conclusion**
  - Mechanical and magnetic centre differ with $(124\ \mu\text{m}, 83\ \mu\text{m})$.
  - The mechanical angle will be verified in the next tests.

Proposed Method: Translating Fluxmeter

- **Basic Principle:**
  A **set of coils** is **pushed longitudinally** through a **constant magnetic field**, inducing a voltage at the terminals as the flux linkage change.

  The signal is mapped to longitudinal position by a **wire-draw encoder**.

  More azimuthal signals can be acquired by **rotating** the fluxmeter.

  The voltage is integrated to **obtain the longitudinal field profile**.

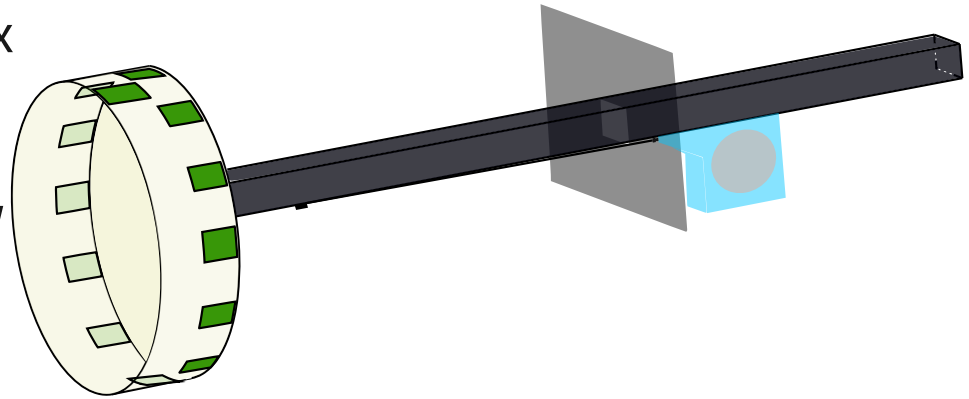

$$U_{ind} = \int_{\partial \mathcal{A}} (\boldsymbol{v} \times \boldsymbol{B}) \cdot d\boldsymbol{r}$$

Translating Fluxmeter: Measurement Setup

The **translating fluxmeter** consists of

- A 3D printed **measurement head**, a **carbon moving rod** and a **guiding tube**
- **13 Printed Circuit Boards** (PCBs) with an active area, $S_{PCB} \approx 0.059\ \mathrm{m}^2$
  - 12 positioned with 30° mechanical displacement.
  - 1 positioned 15° mechanically displaced: reference when the probe is rotated.
- **13 FDIs**
- A **SICK® PFG08-P1AM03PP Wire Draw Encoder**: Resolution 0.014 mm, repeatability ≤0.3 mm, accuracy (linearity) ≤2 mm/3 m.
- **Power Supply**: 6221 Keithley® AC and DC Current Source, $\hat{I} = 105 \pm 0.01$ mA, Offset $\pm\ 0.4$ mA

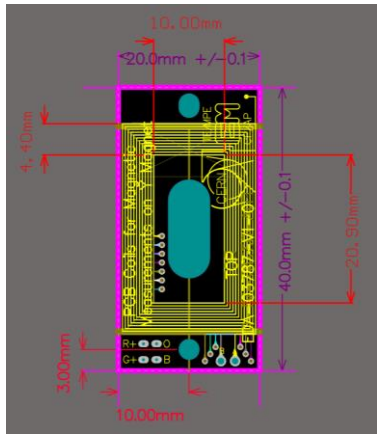

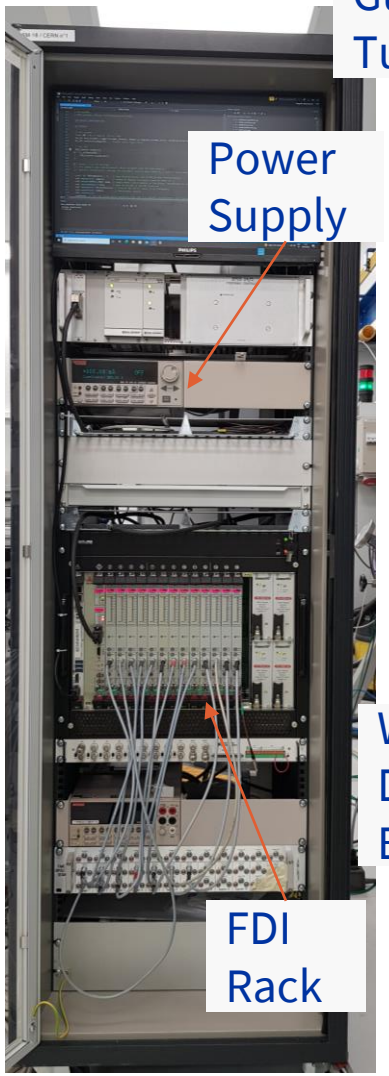

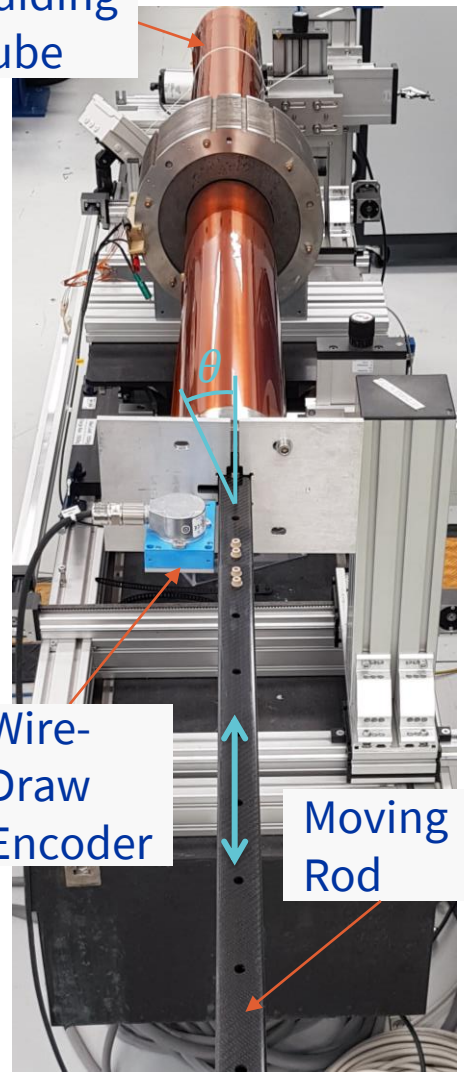

Fluxmeter Analysis: Initial Measurement

Initial Measurement:
Investigate whether the signal is good enough to continue with this set-up.

Result:
The resulting signal strength is sufficiently good.

Next Step:

- Deconvolution of the signal with the PCB sensitivity function.
- Better visualization in space.

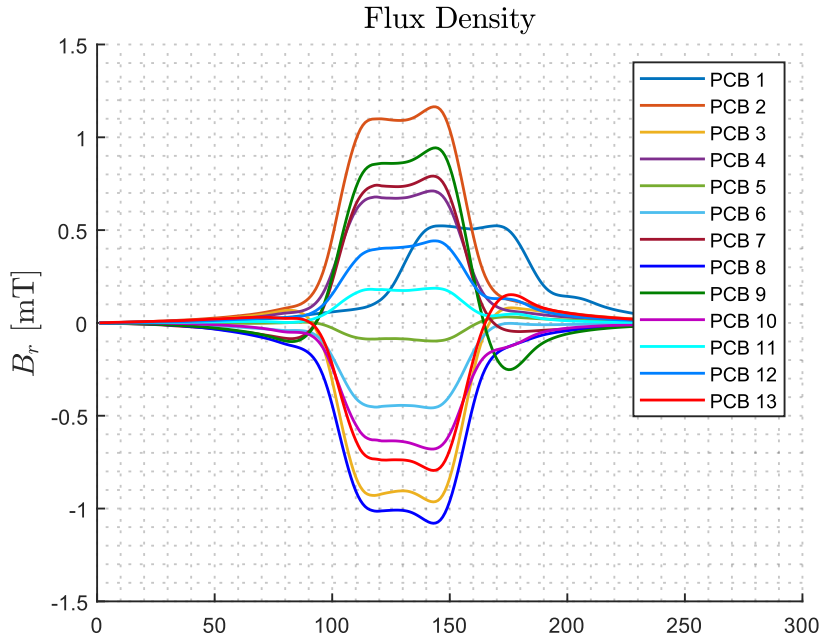

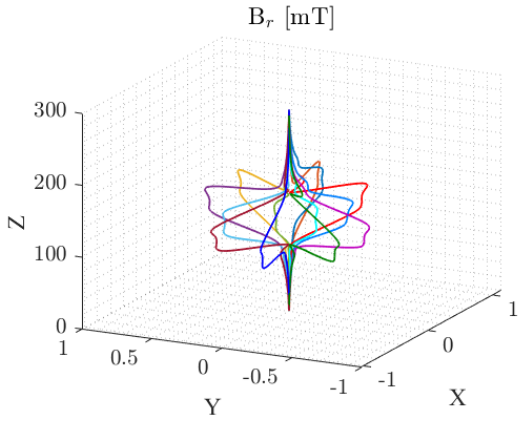

Further Steps

- Additional improvements of the translating fluxmeter and accuracy tests of the wire-measurements.
- Measure the entire corrector package.

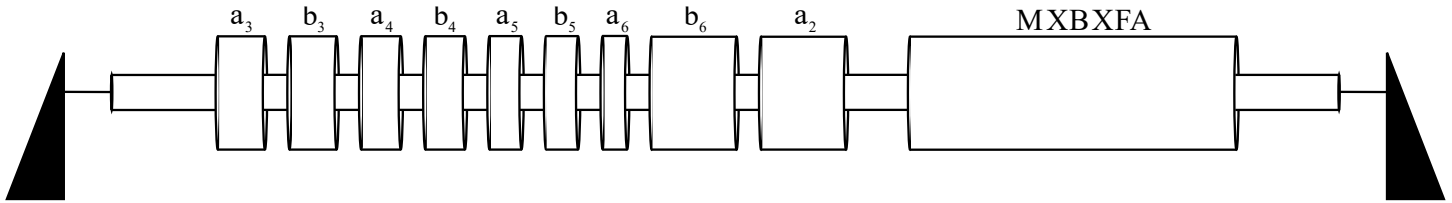

  - The nested dipole in the figure is NOT the MXBXFA, but the MXBXFB.

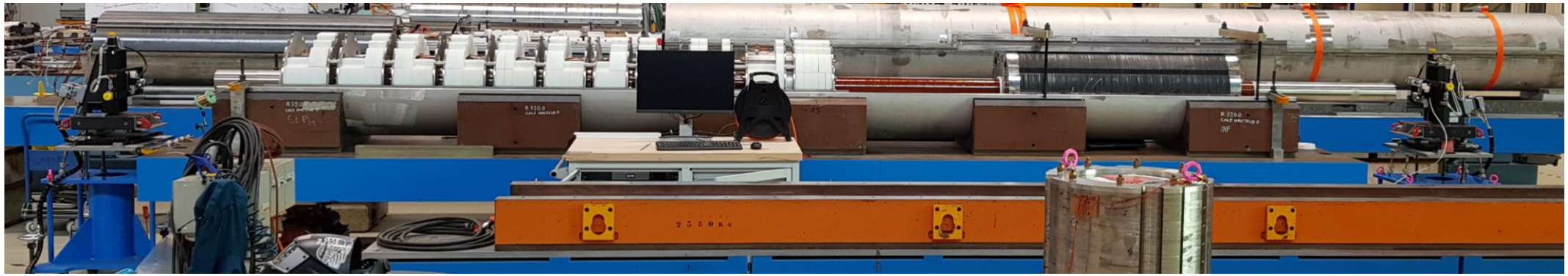

Many thanks to

- Carlo
- Arne
- Lucio
- Guy
- Matthias
- Richard
- Fatiha
- Maxim
- David
- Jose

References

1. S. Russenschuck, *Field computation for accelerator magnets: Analytical and numerical methods for electromagnetic design and optimization*. Weinheim: Wiley VCH Verlag GmbH, Mar. 2010, ISBN: 3527407693.

2. G. Arduini et al., *Chapter 2: Machine Layout* in *High-Luminosity Large Hadron Collider (HL-LHC): Technical design report*, I. Béjar Alonso et al. (Eds.), CERN-2020-010 (CERN, Geneva, 2020), pp. 17-46, doi:10.23731/CYRM-2020-0010.17.

3. E. Todesco, P. Ferracin, *Chapter 3: Insertion Magnets* in *High-Luminosity Large Hadron Collider (HL-LHC): Technical design report*, I. Béjar Alonso et al. (Eds.), CERN-2020-010 (CERN, Geneva, 2020), pp. 47-64, doi:10.23731/CYRM-2020-0010. 47.

4. M. Giovannozzi, S. Fartoukh, R. De Maria, *Initial Models of Correction Systems*, CERN-ACC-2014-0010 (CERN, Geneva, 2014), http://cds.cern.ch/search?p=CERN-ACC-2014-0010

5. R. de Maria, *Engineering Specification - Alignment and mechanical tolerances for HL-LHC in Point 1 and 5*, Rev. 1.0, LHC-G-ES-0023 (CERN, Geneva, 2021), EDMS NO. 2458050.

6. C. Petrone, 'Wire methods for measuring field harmonics, gradients and magnetic axes in accelerator magnets,' Ph.D. dissertation, Università degli Studi del Sannio, 2013, https://cds.cern.ch/record/1601973.

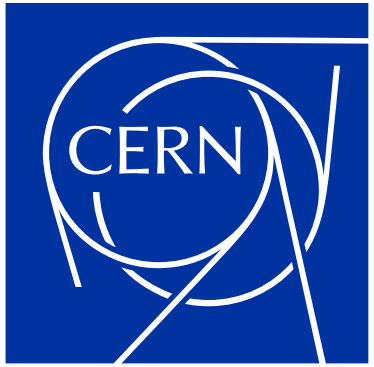

home.cern